SIMULATIONS AND EXPERIMENTAL TESTS ON THE DISTRIBUTION OF OVER-VOLTAGE WITHIN TRANSFORMER WINDINGS

Silviu Gabriel BONȚIDEAN[1], Mihai BĂDIC[2], Mihai IORDACHE[3], Neculai GALAN[4]

*Voltage distribution along the transformer winding for an overvoltage, which reaches the transformer terminals, is studied by simulation with **SYSEG** and by experimental tests. In this purpose, the winding of the transformer is equalled with a power grid made of several flat coils with concentrated electrical parameters and considered known; mutual inductances are not considered; this power grid is used for simulations. These models can be also extended when mutual inductances are added, used in the design stage of the transformer, when all the geometrical sizes are known and electrical parameters may be calculated; this is for an appropriate designation of the winding insulation.*

The experimental tests aim at evidencing the influence of overvoltage and on the adjacent windings in order to consider them in a general power grid. In this study stage, we consider that all the coils have the same electrical parameters.

By knowing the inherent values, we reach a consistent analysis of free oscillations; all the coils have the same electrical parameters and therefore, the free oscillations have close frequencies, the presence of resistance leading to their attenuation.

Keywords: overvoltage, equivalent schemes, simulation, transformer, inherent values

1. Introduction

The overvoltage with rapid change (ORC) or very rapid (OVRC) are the main causes that endanger the insulation of the transformer windings; the detailed study models for the determination of this overvoltage are used since the design stage of the transformer, this way the features of the insulation that can be used may be provided. Under these circumstances, the distribution of voltage along the winding is strongly unequal and the voltage between spires may exceed the accepted voltage of the insulation.

[1] PhD Student, Faculty of Electrical Engineering, University POLITEHNICA of Bucharest, Romania, e-mail: Gabriel_bontidean@yahoo.com
[2] PhD eng., National Institute for R&D in Electrical Engineering ICPE-CA Bucharest, Romania
[3] Prof., Faculty of Electrical Engineering, University POLITEHNICA of Bucharest, Romania
[4] Prof., Faculty of Electrical Engineering, University POLITEHNICA of Bucharest, Romania

Notable that there was still, for a long time in our country, concerns about the behavior of transformers windings subject surges, with remarkable results published in the literature. Original theoretical contributions which were checked on a physical model developed by the author on the distribution of surge along the transformer winding and the analysis of free oscillations are treated in the paper [15].

Although several studies have been published in this field, [1 - 16], because of the complexity of the physical phenomena taking place in the transformer, the results obtained in modelling the transformer for the analysis of free oscillations are still unsatisfactory in terms of concordance between experimental data and theoretical results or the degree of generality of the study models used. This fact is also explained by the large diversity of the types if windings used for transformers and the difficulties regarding the determination of the electrical parameters for the used model (also referred to as equivalent electrical scheme).

2. The equivalent scheme of the three-phase transformer subject to overvoltage

The transient processes in overvoltage take place with a very rapid variation in time and therefore, the equivalent electrical schemes, deduced for the normal operating condition, are no longer valid, [19], [20].

Besides the inductances and resistances, there are also the capacities between the winding spires (longitudinal), between the winding spires and the ferromagnetic core (transversal), as also the conductance between windings and the ferromagnetic core. For a three-phase transformer, the equivalent scheme for transient conditions is more complicated compared to a single-phase transformer, [12], because the transformer window has two high-voltage windings (e.g. A-X and B-Y) and two low-voltage windings (e.g. a-x and b-y) In Fig. 1 we have the equivalent scheme for the single-phase transformer, [12]; the meaning of the parameters results from Fig. 1.

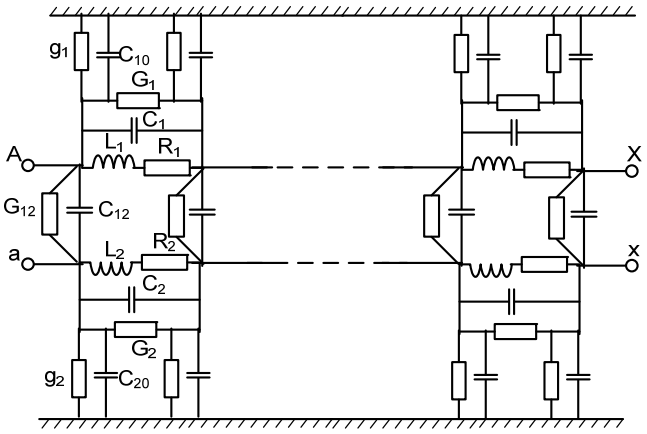

Fig. 1. Equivalent scheme of the windings of single-phase transformer subject to overvoltage

It is worth noting that the structure of the equivalent scheme is also kept if the winding is divided in several coils (RLC Ladder Network model), just that the parameters have different values depending on the gauge of winding division. The parameter values may be close if we take as unit of length the centimetre and the coil by discrete division has the height of a centimetre or the unit of length is the height of the coil through discrete division. In this case, the equivalent scheme is given as a power grid with the items R, L and C, which are studied by means of special calculation software. The RLC Ladder Network model has the advantage that it allows the study of the in-time variation of the electrical sizes of status for every component of the power grid [12].

3. Principles and study methods for overvoltage on transformers

3.1. Overvoltage study methods

The studies on overvoltage, in a large number in the special literature, are interesting because once applied, they increase the operating safety of the transformer.

The calculation models given in the special literature are divided in two categories: Gray Box and Black Box. The Gray Box model includes the mathematical model appropriate to the long lines with distributed parameters (PDM).

The Gray Box model is used in design for the study of behaviour to resonance of the transformer winding evidencing the distribution of voltage along such winding; this model has two options: RLC Ladder Network and multiconductor transmission line – MTL.

The option RLC Ladder Network is a model with parameters R, L, C concentrated; in the original option, it was limited to frequencies of hundreds of

kilohertz, then it was extended to a few megahertz by a spire-to-spire modelling instead of flat-coil modelling. For power and high-voltage transformers, the spire to spire modelling is very complicated and it has difficulties in simulation, [1], [2], [3]. Similar models are used for the study of overvoltage in rotary engines, [4], [5].

The Black Box is useful for coordinating the insulation of the power systems and it can be used to assess the waveform of the current and voltage at the terminals of the transformer, usually based on measurements in time and/ or frequency. This method is usually applied after the transformer was made and is to be commissioned, [6 - 9].

The RLC Ladder Network is the most representative for the study of the transient condition on overvoltage for the possibilities it offers in building equivalent schemes of the transformer windings. RLC Ladder Network is given in Fig. 2.

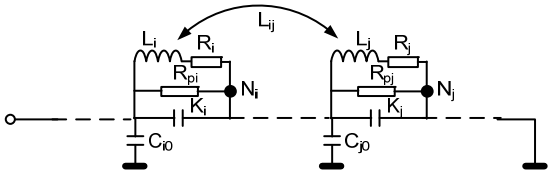

Fig. 2. RLC Ladder Network

The main element of this model is the disk coil; the three sides of the disk coil noted i are connected in parallel and against the ground the coil has the capacity C_{i0}; R_i and L_i, serial connected, resistance and inductance of the coil, K_i it is an equivalent capacity made of the coil spires, and the resistance R_{pi} represents the losses in the insulator. There are only considered the mutual inductances between the disk coils, between coil i and coil j the mutual inductance is L_{ij}; the mutual inductances between the spires of the same coil are neglected, this way the model is much simpler. Based on the equations of Kirchhoff, it is established the matrix equation between currents, voltages and operating impedance regarding the N kinks.

The MTL model consists in a grid with N conductors all connected together, characterised by a matrix [L] made of inductances and a matrix [C] made of capacities (capacities C_{ii} between spire i and ground; the capacities between spire i and spire j taken with negative sign, for $i \neq j$; the capacities C_0 between each spire of the winding and mass - forms the matrix diagonal). In Fig. 3 it is given the multiconductor line transmission model (MTL). If the number of spires is higher, disk coils are formed with a low number of spires (spire to spire consideration would lead to a large working volume without reaching significant calculation accuracy). The parameters of the spires or of the disk coils may be

different (due to consolidating the insulation of the first spires from transformer winding, slightly different diameters etc.). In all cases, the following relations between voltages *u* and currents *i* remain valid:

$$u_{ri} = u_{s(i+1)}; \quad i_{ri} = i_{s(i+1)} \tag{1}$$

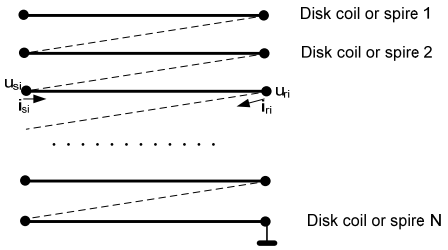

Fig. 3. Multiconductor transmission model (MTL)

In this stage there are two ways that can be used.

a) The model where the disk coil can be considered as a MTL model and represents an extended transmission line, noted MTLM (each spire of the coil represents a transmission line, fig. 4). The spires of each disk coil, generally, are not identical and each spire can be equalled with a long transmission line. For identical spires or disk coils, the model is much simpler.

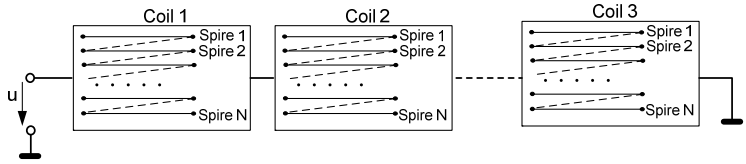

Fig. 4. The MTLM model.

b) The model where each disk coil is equalled with a transmission line with a single conductor in the form of a transmission line, noted STLM (the serial spires represent a transmission line, fig. 5). The spires of each coil are equalled with a single conductor.

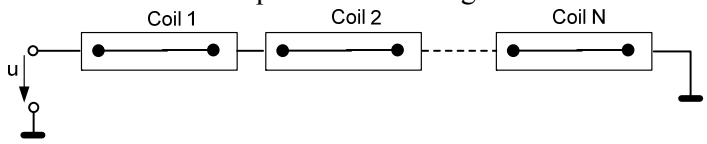

Fig. 5. The STLM model.

In both cases, based on theorems of Kirchhoff, mathematical models are established, which are similar to the mathematical model corresponding to long lines, i.e. the differential equations of the models MTLM and STLM, originating

in the equations of telegraphists. These models are used to study the overvoltage with very rapid variation in time, which occur because of the commutations in the grid; some of them have a very sharp front and are dangerous for the transformer winding. MTLM and STLM have led to a good consistency between the calculated and measured data. A major problem in solving the wave equation in time consists in the fact that the line parameters, particularly the resistance and inductance, depend on frequency [7]. The aforementioned models can be synthesised in the scheme from Fig. 6.

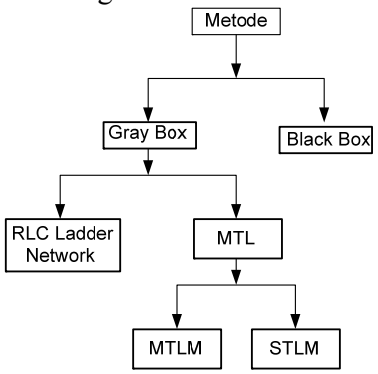

Fig. 6. Methods used in the study of overvoltage

These methods usually apply combined; in majority of the cases, RLC Ladder Network is elaborated and then each coil from the network is analysed by MTLM or STLM method, depending on the pursued purpose (MTLM on design, STLM on the study of voltage distribution on a given transformer with the use of experimental data). The two options of the MTL method use the mathematical model corresponding to long lines with distributed parameters (PDM), which is based on the equation of the telegraphists. The presented models (fig. 6) are applied as various forms for different transformers depending on the construction of the windings. Each of the methods has arguable items and due to this, completions are brought in the applications. In all the methods, the essential issue is the one of the electrical parameters for which determination different calculation modalities have been formulated.

3.2. The parameters of the mathematical models.

The main parameters are: the resistance of the coil or of the spire – R; the capacities appearing in the model – C; the resistance of the insulating material– R_I; the inductances of the coils or spires – L. For PDM model, the line parameters are calculated, i.e. the electrical parameters on the length unit,

A. The capacity on unit of length, as element of a matrix, can be calculated with the method of the finite element (FEM). It is assumed that there are N

conductors; and the conductor j i applies the voltage of 1V, the other conductors are on zero potential. [10]. The relations used in this purpose are:

$$C_{ij} = \frac{q_i}{\Delta U_{ij}}, i \neq j\,; \quad W_j = \frac{1}{2}\sum_{i=1}^{N} C_{ij}\Delta U_{ij}^2 \tag{2}$$

Where: C_{ij} - capacity between the conductor i and the conductor j; q_i – the electrical load on the conductor i; ΔU_{ij} – difference of potential between the conductor i and the conductor j; W_j – the energy of the electrostatic field of the system. W_j can be easily calculated with FEM software package. This method can be exemplified with the rectangular conductor system given in Fig. 7.a. Voltage is applied to conductor 5 and the energy of the electrostatic field W_5 is calculated, similarly as with the conductor 4 and W_4 is calculated, when conductor 8 and we obtain W_8. Given this, the following equations are established:

$$\begin{aligned}
&\frac{1}{2}C_s\Delta U_{52}^2 + \frac{1}{2}C_s\Delta U_{58}^2 + \frac{1}{2}C_k\Delta U_{54}^2 + \frac{1}{2}C_k\Delta U_{56}^2 = W_5\,;\\
&\Delta U_{52} = \Delta U_{58} = \Delta U_{54} = \Delta U_{56} = 1V;\\
&\frac{1}{2}C_s\Delta U_{41}^2 + \frac{1}{2}C_s\Delta U_{47}^2 + \frac{1}{2}C_k\Delta U_{45}^2 + \frac{1}{2}C_g\Delta U_{40}^2 = W_4\,;\\
&\Delta U_{41} = \Delta U_{47} = \Delta U_{45} = \Delta U_{40} = 1V;\\
&\frac{1}{2}C_s\Delta U_{85}^2 + \frac{1}{2}C_k\Delta U_{87}^2 + \frac{1}{2}C_g\Delta U_{89}^2 = W_8\,;\\
&\Delta U_{85} = \Delta U_{87} = \Delta U_{89} = 1V
\end{aligned} \tag{3}$$

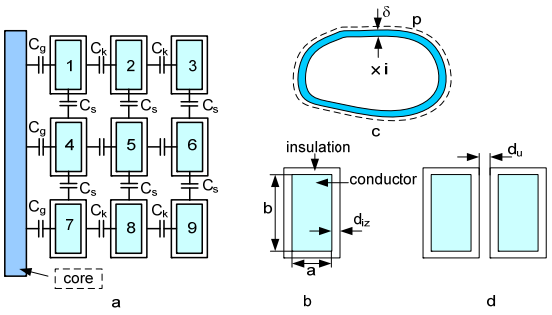

Fig. 7. a) Arrangement of the conductors of a part from the transformer winding; b) details with regard to the conductor; c) conductor with a given section crossed by the current i; d) the positioning of two conductors for the calculation of capacity. a and b are the sizes of the rectangular conductor, d_{iz} – thickness of the conductor insulation, d_u – thickness of the oil layer between conductors, p – conductor perimeter, δ - thickness of the penetration depth for a net Kelvin effect.

Based on the equations (3), it is formed the matrix equations (4) and the capacities C_s, C_k and C_g are calculated, which are the unknown of the equation.

$$\begin{vmatrix} 1 & 1 & 0 \\ 1 & 0,5 & 0,5 \\ 0,5 & 1 & 0 \end{vmatrix} \cdot \begin{vmatrix} C_s \\ C_k \\ C_g \end{vmatrix} = \begin{vmatrix} W_5 \\ W_4 \\ W_8 \end{vmatrix} \tag{4}$$

This way, the capacities between spires or between spires and mass are more accurate calculated because the end effect is no longer neglected, this being very important to these conductor sizes. With the values of the capacities calculated, the matrix $|C|$ is calculated.

The capacity between two conductors can be calculated with simple relations if the end effect is neglected (the electric field is uniform between the two conductors), for example we consider the conductors from Fig. 7.d. Knowing that the normal component D_n of the electrical induction is conserved at the separation surface of two media, then the necessary relations to determine the capacity between the two conductors can be written:

$$\begin{aligned} &D_{niz} = \varepsilon_{iz} E_{niz} = \varepsilon_u E_{nu} = \frac{q}{A}; \quad A = b \cdot l; \\ &U = 2\, d_{iz}\, E_{niz} + d_u\, E_{nu} \Rightarrow C = \frac{q}{U} = \frac{A}{\frac{2\, d_{iz}}{\varepsilon_{iz}} + \frac{d_u}{\varepsilon_u}}; \\ &C = \frac{A}{\sum_{i=1}^{n} \frac{d_i}{\varepsilon_i}} \end{aligned} \tag{5}$$

where D_n and E_n are the normal components of the electrical induction and respectively the intensity of the electric field; l is the conductor's length; q is the electric load; U is the voltage between the faces of the two conductors. In relation 5, it was also given the general expression of a plain condenser where the insulation between plates is made of n plain statures with different dielectric constants ε_i.

B. The resistance on length unit should be calculated considering the net Kelvin effect taking place on high frequencies or on rapid variations of the current i which crosses the conductor. On net Kelvin effect, the electricity i is distributed on the conductor surface on the penetration depth δ (fig. 7.c); for a given surface of the conductor section, resistance $R\delta$is calculated, and for the rectangular surface, the resistance R_{dr} is calculated.

The calculation relations are:

$$R_\delta = \frac{1\cdot\rho}{p\,\delta};\quad \delta = \sqrt{\frac{2\,\rho}{\omega\,\mu}} = \sqrt{\frac{1}{\pi\,\sigma\,f\,\mu}} \Rightarrow$$
$$R_\delta = \frac{1}{p}\sqrt{\frac{\pi\,f\,\mu}{\sigma}};\quad R_{dr} = \frac{1}{2(a+b)}\sqrt{\frac{\pi\,f\,\mu}{\sigma}};\quad \rho = \frac{1}{\sigma} \tag{6}$$

ρ and μ are the electrical resistivity and magnetic permeability of the conductor material, for copper $\mu = \mu_0$.

C. The inductance on length unit L_l is more difficult to calculate, this inductance has two components; one component, noted with L_e, refers to the magnetic field from outside the conductor, and the other component, noted with L_i, refers to the magnetic field from inside the conductor. For the component L_e m we use the propagation speed of the waves v_0**.** The overvoltage waves propagate through dielectric media where $\mu = \mu_0$ and $\varepsilon = \varepsilon_0\,\varepsilon_r$, ε_r is the dielectric constant of the medium. In this case, the dielectric only changes the capacity value, and the following relations can be established:

$$v_0 = \frac{1}{\sqrt{L_l\,C_l}} = \frac{1}{\sqrt{L_l\,C_{l0}\,\varepsilon_r}} = \frac{c}{\sqrt{\varepsilon_r}} \Rightarrow \underline{L_l = \frac{\varepsilon_r}{c^2\,C_l} = L_e};$$
$$C_l = \frac{A\,\varepsilon}{d} = \frac{A\,\varepsilon_0\,\varepsilon_r}{d} = C_{l0}\,\varepsilon_r;\quad C_{l0} = \frac{A\,\varepsilon_0}{d};\quad c = \frac{1}{\sqrt{L_l\,C_{l0}}} \tag{7}$$

where c is the speed of light determined by the constants μ_0 and ε_0; irrespective of the condenser geometry. C is proportional with the electric constant $\varepsilon = \varepsilon_0\,\varepsilon_r$ and then we can write the relation $C = C_0\,\varepsilon_r$ where C_0 sis determined by ε_0. The capacity C_l can be relatively easy determined from the relation (7), resulting the inductance L_e (the underlined relation).

To calculate the component L_i we use the results obtained in the case of penetration of the electromagnetic field in the conducting semi-infinite space; it is considered a rectilinear cylindrical conductor, with the area of the transversal section S, if the condition $\delta << S^{1/2}$ is fulfilled, then the Kelvin effect is net. For the net Kelvin effect, the expression of the wave impedance $\underline{Z}$ has the real part R equal with the imaginary part ωL, obtaining:

$$\underline{Z} = \frac{\underline{E}}{\underline{H}} = R + j\,\omega\,L;\quad R = L;\quad R = R_S;$$
$$L = L_i \Rightarrow L_i = \frac{R_S}{\omega} = \frac{R_S}{2\,\pi\,f} \tag{8}$$

i.e. on a given pulsation, ω the inductance L_i is calculated with the resistance R_s, which was calculated. The inductance L_l is: $L_l = L_e + L_i$.

For a more precise calculation, it is considered the physical model from Fig. 8, where the core of radius a is considered of infinite length [11], fact

justified by the ferromagnetic core of the transformer, which forms a closed loop, and the end effects can be neglected. It is considered that the core (noted 1; $r \le b$) has magnetic anisotropy (the transformer core is made of cold-laminated sheet iron) and therefore the magnetic permeability μ_r after direction *0r* and μ_z after direction *0z* are different, the conductivity of medium *1* is σ. Other data are given in Fig. 8.

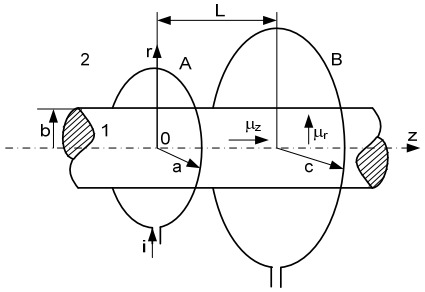

Fig. 8. Filamentary spires arranged concentrically on the ferromagnetic core.

Unlike the work [11], it is ought to establish the differential equation with partial derivations of the vector magnetic potential produced by the current *i*. For this magnetic field with axial symmetry, the vector magnetic potential, in cylindrical coordinates (r, α, z), has only one component different from zero, i.e. the component $A\alpha$, which makes the calculations much simpler. The magnetic field having axial symmetry, the component Aα depends only on the coordinates r and z, i.e. $A\alpha$(r,z).

The following vector equations are considered:

$$\vec{B} = rot\,\vec{A}\,; \quad div\,\vec{A} = 0\,; \quad rot\,\vec{H} = \vec{J} \tag{9}$$

The magnetic field having axial symmetry, the equation of component $A\alpha$ of the vector magnetic potential is deduced, considering that the Krarup core is magnetically anisotropic: μ_r is the magnetic permeability after the direction r, and μ_z is the magnetic permeability in the direction z.

The equation of component $\underline{A}\alpha_1$ of the vector magnetic potential, in area 1, for the sinusoidal variation in time is:

$$r \le b\,; \quad \frac{1}{r}\frac{\partial}{\partial r}\left(r\frac{\partial \underline{A}_{\alpha 1}}{\partial r}\right) + \frac{1}{a^2}\frac{\partial^2 \underline{A}_{\alpha 1}}{\partial z^2} = j\omega\mu_z\sigma\,\underline{A}_{\alpha 1\alpha}\,;$$
$$a = \sqrt{\frac{\mu_r}{\mu_z}}\,; \quad \gamma^2 = j\omega\mu_z\sigma\,; \tag{10}$$

For area 2 *(r ≥ b)*, the magnetic potential $A\alpha_2$ can be put under the form:

$$\underline{A}_{\alpha 2} = \underline{A}'_{\alpha 2} + \underline{A}''_{\alpha 2}$$

$$r \geq b; \quad \frac{1}{r}\frac{\partial}{\partial r}\left(r\frac{\partial \underline{A}'_{\alpha 2}}{\partial r}\right) + \frac{1}{a^2}\frac{\partial^2 \underline{A}'_{\alpha 2}}{\partial z^2} = 0; \tag{11}$$

$$r \leq a; \quad A_{\alpha 2} = \frac{\underline{I}\,\mu_0}{\pi}\int_0^{\infty} K_1(\lambda a) I_1(\lambda r)\cos\lambda z\, d\lambda$$

where I_1(x) and K_1(x) are the modified Bessel functions of 1st and 2nd order.

By using the method of variable separation, the component $\underline{A}\alpha_i$ (i = 1; 2) can be put under the form:

Component A_{zi} is given for the two fields 1 and 2 as the product of two functions R(r) and Z(z) according to the method of variable separation and two differential equations are obtained:

$$A_{\alpha i} = A_{\alpha i}(r, z) = R_i(r)\, Z_i(z) = R_i\, Z_i; \quad i = 1; 2,$$

$$\frac{1}{R_i}\left(\frac{d^2 R_i}{d r^2} + \frac{1}{r}\frac{d R_i}{d r}\right) - \gamma^2 = -\frac{1}{a^2}\frac{1}{Z_i}\frac{d^2 Z_i}{d z^2} = \lambda^2 \Rightarrow \tag{12}$$

$$\Rightarrow \begin{cases} \dfrac{d^2 R_i}{d r^2} + \dfrac{1}{r}\dfrac{d R_i}{d r} - \left(\gamma^2 + \lambda^2\right) R_i = 0 \\ \dfrac{d^2 Z_i}{d z^2} + \lambda^2 a^2\, Z_i = 0 \end{cases}$$

The first differential equation from (12) is a Bessel equation. The solutions of the two differential equations are:

$$zone\,1 \Rightarrow \begin{cases} R_1(r) = P_{\lambda 1} I_1\left(r\sqrt{\gamma^2 + \lambda^2}\right) + R_{\lambda 1} K_1\left(r\sqrt{\gamma^2 + \lambda^2}\right); \\ Z_1(z) = S_{\lambda 1}\cos(\lambda a z) + T_{\lambda 1}\sin(\lambda a z) \end{cases}$$

$$zone\,2, \gamma = 0; \Rightarrow \begin{cases} R_2(r) = P_{\lambda 2} I_1(r\lambda) + R_{\lambda 2} K_1(r\lambda); \\ Z_2(z) = S_{\lambda 2}\cos(\lambda z) + T_{\lambda 2}\sin(\lambda z) \end{cases} \Rightarrow \tag{13}$$

$$\Rightarrow A'_{\alpha 2} = R_2(r)\, Z_2(z)$$

The conditions of surface crossing are inserted, $r = b$, to determine the integration constants; there are two conditions:

1. The preservation of the tangential components of the intensity of the magnetic field with considering the current J_s from the discontinuity surface, can be provided by means of the axial component $A\alpha$ of the vector magnetic potential calculated for the two areas:

$$H_{t1} - H_{t2} = H_{z1} - H_{z2} = J_s \Leftrightarrow \frac{1}{\mu_z}\frac{\partial A_{\alpha 1}}{\partial r}\Big|_{r=b} - \frac{1}{\mu_0}\frac{\partial A_{\alpha 2}}{\partial r}\Big|_{r=b} = J_s \; ; \qquad (14)$$

2.The preservation of the normal components of induction can be provided by means of the axial component A_z of the vector magnetic potential:

$$B_{n1} = B_{n2} = B_{r1} = B_{r2} \Leftrightarrow \frac{\partial A_{\alpha 1}}{\partial z}\Big|_{r=b} = \frac{\partial A_{\alpha 2}}{\partial z}\Big|_{r=b} \qquad (15)$$

With the relations (14) and (15) and considering the singularities of the Bessel functions, the integration constants are determined. $P\lambda$, $R\lambda$, $S\lambda$ and $T\lambda$.

To calculate the inductances L_{AA} and L_{AB} the following relations are used:

$$L_{AA} = \frac{1}{i}\iint_{S_\Gamma} \vec{B}\,\overrightarrow{dS} = \frac{1}{i}\iint_{S_\Gamma} rot\,\vec{A}\,\overrightarrow{dS} = \frac{1}{i}\int_{\Gamma} \vec{A}\,\overrightarrow{ds} = \frac{1}{i}\int_{C(a-r_c)} A_{\alpha 2}(a - r_c, 0)\, a\, d\,\alpha \; ;$$
$$ds = a\, d\alpha; \qquad L_{AA} = \frac{1}{i}\int_{C(b)} A_{\alpha 2}(b, L)\, a\, d\,\alpha \qquad (16)$$

The inductance L_{AA} is calculated by using as curve Γ the circle with radius $a - r_c$, meaning $C(a\text{-}r_c)$ to remove the discontinuity on $r = a$, r_c is the radius of spire A. For the inductance L_{AB} the curve is the circle C(b)

In the case of several spires, we use the superposition principle; analytic relations expressed by Bessel functions are obtained. These inductances can be also calculated by the method of the finite element (FEM).

D. The conductance G of the insulating material depends on pulsation, ω, capacity C and on the loss factor, tgδ; according to [10], it is calculated with the relation:

$$G = \omega\, C \tan\delta = 2\pi\, f\, C \tan\delta \qquad (17)$$

4. The simulations regarding the distribution of overvoltage along the transformer winding with the null on ground, using the *RLC* schemes

The model RLC Ladder Network is adopted, consisting in dividing the high-voltage winding in disk coils with concentrated parameters (paragraph 3.1), an equivalent scheme (power grid) of the high-voltage winding is obtained.

In this scheme (fig. 9), there are considered the resistances and inductances of the disk coils together with the capacities formed by the winding spires (between spires and ground spires), and the software SYSEG applies [14]. It is considered that on the terminals of the winding, the overvoltage e_1 is a pitch voltage, $e_1 = 10$ u.r. This overvoltage, in the initial moment, has a gradual increase and it leads to a strongly unequal distribution of the overvoltage along the

transformer winding. If the wave front is smoother, then the distribution of overvoltage along the winding is less unequal.

In the work [12], it was considered the form overvoltage $e_1 = 20\ [\exp(-t/T_e)-1]$, in this case the distribution of overvoltage along the winding largely depends on the time constant T_e; the more this constant is lower, the more the overvoltage distribution is more prone.

In Fig. 9 we have the RLC scheme for the transformer with null to earth (X is connected to ground) and simulations will be made for $e_1 = 10$ u.r.

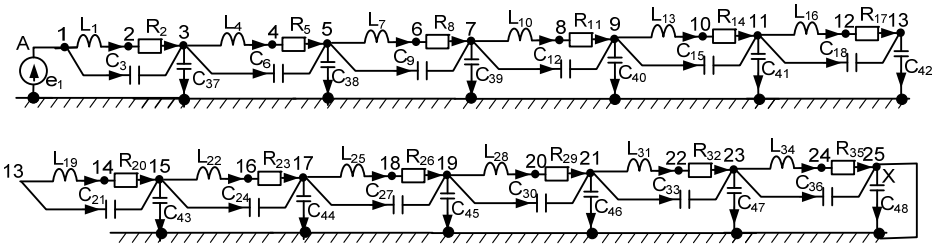

Fig. 9. Scheme of the winding with null to earth.

For the scheme from Fig. 9, it was considered that the disk coils are identical, i.e. each coil has the same electrical parameters. This simpler scheme has the advantage that it facilitates the physical interpretation of the obtained results.

For the electrical parameters, the same values as in work [12] are kept:

$$\begin{aligned} &L_1=L_4=L_7=L_4=L_{10}=L_{13}=L_{16}=L_{19}=L_{22}=L_{25}=L_{28}=L_{31}=L_{34}= 4\cdot10^{-6}\ \text{H} \\ &R_2=R_5=R_8=R_{11}=R_{14}=R_{17}=R_{20}=R_{23}=R_{26}=R_{32}=R_{35}= 2\cdot10^{-3}\ \Omega \\ &C_3=C_6=C_9=C_{12}=C_{15}=C_{18}=C_{21}=C_{24}=C_{27}=C_{30}=C_{33}=C_{36}= 30\ \text{pF} \\ &C_{37}=C_{38}=C_{39}=C_{40}=C_{41}=C_{42}=C_{43}=C_{44}=C_{45}=C_{46}=C_{47}=C_{48}= 90\ \text{pF} \end{aligned} \tag{18}$$

The numeric data with regard to the own values are:

$$\begin{aligned} \textit{Valori\_proprii} := \{ & -499.9999999999994\ ,\ -250.0000000000006\ -\ 0.4564354645807917\ 10^8\ I,\ -250.0000000000006\ +\ 0.4564354645807917\ 10^8\ I, \\ & -250.0000000000004\ -\ 0.5249682534639905\ 10^8\ I,\ -250.0000000000004\ +\ 0.5249682534639905\ 10^8\ I, \\ & -250.0000000000003\ -\ 0.3689664035954784\ 10^8\ I,\ -250.0000000000003\ +\ 0.3689664035954784\ 10^8\ I, \\ & -250.0000000000002\ -\ 0.2613954087961587\ 10^8\ I,\ -250.0000000000002\ +\ 0.2613954087961587\ 10^8\ I, \\ & -250.0000000000001\ -\ 0.1360500996321295\ 10^8\ I,\ -250.0000000000001\ +\ 0.1360500996321295\ 10^8\ I,\ -250.\ -\ 0.6875167903875110\ 10^8\ I, \\ & -250.\ -\ 0.6166367751086538\ 10^8\ I,\ -250.\ +\ 0.6166367751086538\ 10^8\ I,\ -250.\ +\ 0.6875167903875110\ 10^8\ I, \\ & -250.0000000000000\ -\ 0.6454972243630613\ 10^8\ I,\ -250.0000000000000\ +\ 0.6454972243630613\ 10^8\ I, \\ & -249.9999999999999\ -\ 0.6660134667804056\ 10^8\ I,\ -249.9999999999999\ -\ 0.5773502691842127\ 10^8\ I, \\ & -249.9999999999999\ +\ 0.5773502691842127\ 10^8\ I,\ -249.9999999999999\ +\ 0.6660134667804056\ 10^8\ I, \\ & -249.9999999999996\ -\ 0.6796877743131910\ 10^8\ I,\ -249.9999999999996\ +\ 0.6796877743131910\ 10^8\ I \} \end{aligned} \tag{19}$$

The inherent values are approximately the same as with the winding of the insulated null (the difference also explains by the fact that by grounding, the condenser is not short-circuited C_{48}) but there appears a new inherent value with null imaginary part because by grounding the winding, a circuit *RL* is formed, where only the time constant *L/R* appears. These inherent values are determined only by the parameters of the equivalent schemes.

The inherent values V_P are given under the form of a complex number out of which it results the time constant *T* and the pulsation ω:

$$V_p = a + j\,b\,; \quad T = \frac{1}{a}; \quad \omega = b \tag{20}$$

4.1. Main description of the software SYSEG

SYSEG is capable of providing the status equations under symbolic form, symbolic-numerical and numeric form, for a very wide class of linear and/ or non-linear analogue circuits. These circuits may contain: linear and/ or non-linear resistors controlled in voltage (c.u.) or in current (c.c.), linear and/ or non-linear condensers controlled in voltage (c.u.), linear coils (coupled or not magnetically) and/ or non-linear coils controlled in current (c.i.), ideal independent sources of voltage and/ or current, all the four two-port sources and generally any multi-port circuit item having an equivalent scheme made of only two-pole circuit items and operated sources. By reducing and simplifying the expressions, one can obtain a symbolic compact form of the system of status equations. Syseg can identify, as number and type, the items in excess of first category and the ones of second category. SYSEG generates the normal tree, the appropriate equations of the Kirchhoff theorems, the constitutive equations (specific) of the circuit items, creating a file named *script.dat*. This file is called by the Maple simulator, which allows handling of the symbolic expressions and finally it produces the status equations in symbolic form. Additionally, SYSEG has other capabilities, offering the status matrix of the circuit, the matrix of coefficients of the excitation units, the matrix of coefficients of the derivations of excitation units, the matrix corresponding to the output units and to the characteristic polynom in symbolic form, or making the numeric evaluation, in an operating point for the non-linear analogue circuits, of the inherent values or inherent vectors, for various values of the circuit parameters. Hence, the lowest inherent value (or the highest time constant) allows estimation of the total simulation time, and the highest inherent value (or the lowest time constant) facilitates the selection of the dimension of the time step. Obviously, SYSEG finally offers the analysis in time of the circuit for different numeric values of its parameters. Syseg is written in C++ and it constitutes an interactive instrument which combines the techniques of symbolic

and numeric calculation and it uses the facilities of the symbolic simulator Maple, to handle symbolic expression, [14], [17], [18].

4.2. The results obtained after running the software Syseg.

In the following are given the variations in time of the voltages on the capacities C_3, C_6 and C_9, which evidence the distribution of voltage along the winding for the first three coils, Figs. 10, 11 and 12.

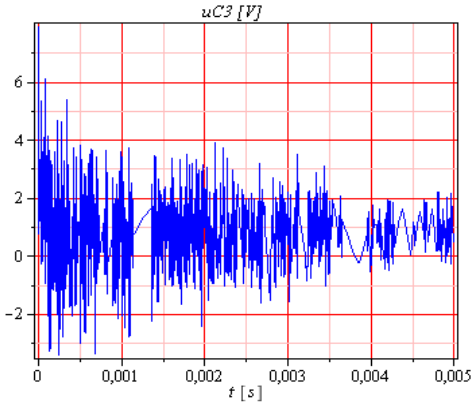

Fig. 10. The variation in time of the condenser voltage C_3.

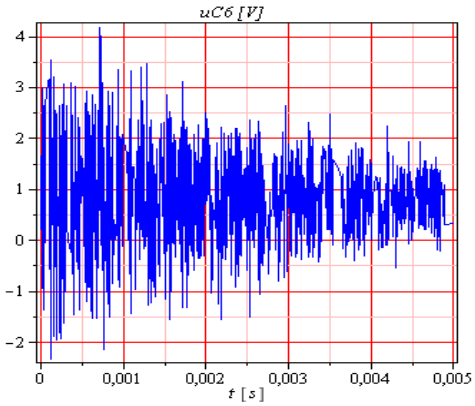

Fig. 11. The variation in time of the condenser voltage C_6.

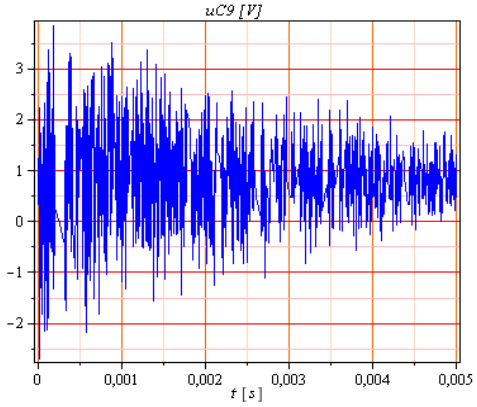

Fig. 12. The variation in time of the condenser voltage C_9.

By analysing the Figs. 10, 11 and 12 it is determined that, in the first moment, the voltage on terminals is largely taken-over by the capacity C_3 (7 u.r from 10) which is also the voltage on the terminals of the first disk coil, after which it drops and peaks of close value no longer appear. On the following coils C_6 and C_9 , the voltages remain high and with close values (approximately 3.5 u.r. from 10), but there should be noted that after the initial moment, peaks of voltage as high or even higher than in the initial moment appear; uC_6 has a voltage of 4.2 u.r. on t = 0.0008 as compared to 3.5 in the initial moment, similar is also the case of capacity C_9, in the initial moment the voltage did not exceed 3 u.r. but shortly there appears a voltage peak of 4 u.r. This is explained by the fact that the voltage expression is represented by a combination of exponential functions and sinusoidal functions according to the inherent values and their algebraic sum on a given time may lead to such values or even to voltage dip as determined on Figs. 10, 11 and 12. In this case, it is a very rapid variation of the voltage on terminals, and therefore the first coils are very stressed, fact known from the special literature, but this representation in time offers information with regard to the moments after the initial moment, when the voltage peaks become dangerous.

5. Experimental trials

In order to confirm some ideas from this work, a few simple experimental have been performed, using the accessible terminals of the transformer windings. Two transformers were used: a single-phase transformer and a low-duty three-phase transformer. As voltage supplie (u), there was used a condenser, which was loaded on a direct current network and the discharged on the transformer winding (high voltage).

5.1. The single-phase transformer

The transformer is a voltage transducer in open configuration and it has the voltages U_{AX} = 1kV; U_{ax} = 100V.

In Fig. 13 is given the voltage applied to the winding AX from the condenser and the voltage on the secondary terminals ax. It is determined that the voltage applied to the AX terminals has a leap at the beginning and it drops in time, approximately after a line (curve 1). The voltage at the ax terminals has an oscillating variation in them, which shows that the voltage is not induced only by the flow produced by the AX winding. If it would be induced by this flow, then the secondary would have a constant voltage after the first moments, because the magnetic flow produced by the primary winding has a linear variation (the magnetic flow from primary varies approximately as the voltage on terminals). Hence, the voltage on secondary is transmitted by the capacities formed between the high-voltage and the low-voltage spires. The form of voltage u_{ax} shows that there are several inherent values for free oscillations.

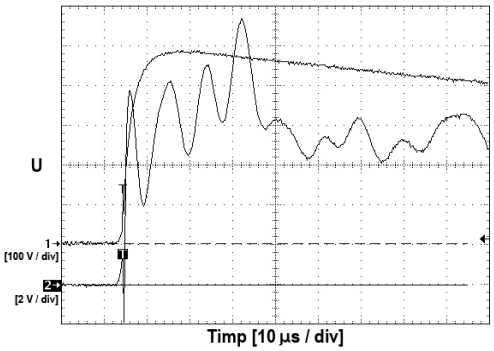

Fig. 13. The variation in time of the voltages u_{AX} (curve 1) and u_{ax} (curve 2).

5.2. The three-phase transformer

The three-phase transformer is in open configuration and it has the voltages 230/400V;

In Fig. 14 is given the voltage applied to the winding BX from the condenser and the voltage on the primary terminals AX. The voltage is transmitted by the capacities formed between the high-voltage spires of the winding BY and the ones of high voltage of the winding AX. The form of voltage u_{AX} shows that there are several inherent values for free oscillations.

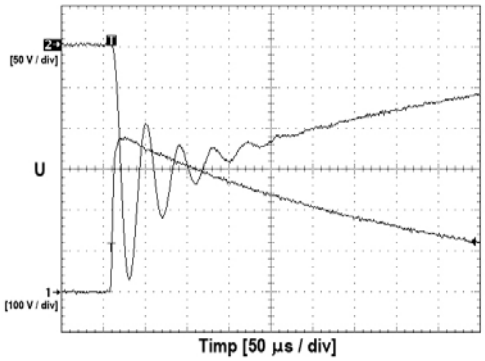

Fig. 14. The variation in time of the voltages u_{BY} (curve 1) and u_{AX} (curve 2); supply from condenser

The trial was repeated for the high-voltage winding CZ; the variation forms are identical because the windings AX and CZ are symmetric in relation with the winding BY.

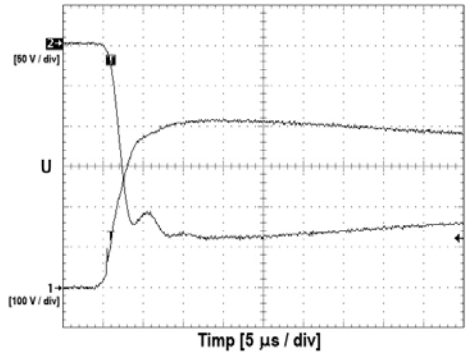

Fig. 15. The variation in time of the voltages u_{BY} (curve 1) and u_{by} (curve 2); supply from condenser.

It was applied the voltage from condenser on the winding BY and the voltage on by was recorded; the same phenomenon is recorded for the presence of free oscillations, but the amplitudes are lower, (Fig. 15).

The trials with high-frequency supply of the transformer winding do not bring new elements with regard to the behaviour of the adjacent winding.

6. Conclusions

A synthesis was elaborated with regard to the methods used for the study of overvoltage on transformers and the calculation of the parameters of the

equivalent power grid. The capacities from the network are relatively simple to calculate, more complicated is to determine the inductances; a possibility consists in using the propagation speed of the overvoltage wage along the winding, another possibility would consist in calculating the spatial distribution of the magnetic field. Within this context, the work showed another way of calculation by using the vector magnetic potential, which at the magnetic field with axial symmetry, in cylindrical coordinates, has a single component different from zero, i.e. the tangential component. In order to take into account the magnetic anisotropy of the Krarup core, the equation of the vector magnetic potential was elaborated for magnetic anisotropy medium. This way, useful relations were established for the calculation of inductances.

Based on the equivalent scheme of the primary winding, with disk coils, the distribution of the overvoltage on the first disk coils was simulated with SYSEG, allowing consistent physical interpretations and explanations for the waveforms obtained through simulation. Knowing the inherent values indicates the structure of the functions, which represent the variation in time of the analysed units.

The experimental part was performed on two transformers: a single-phase transformer and a three-phase transformer. In all the performed trials it is determined that if a high-voltage winding is subject to overvoltage, then voltages of significant values are transmitted also in the adjacent windings. This confirms the reasoning for making an equivalent power grid for the transformer windings, which would also include the electrical parameters of the adjacent windings, as given in Fig. 1; such a power grid shows interest during the design stage of the transformer, when the features of the used materials and the constructive dimensions are known.

REFERENCES

1. *S. M. Hassan Hosseini, Mehdi Vakilian, and Gevork B. Gharehpetian,* Comparison of Transformer Detailed Models for Fast and Very Fast Transient Studies. IEEE TRANSACTIONS ON POWER DELIVERY, VOL. 23, NO. 2, APRIL, pp. 733 – 741 2008.
2. *B. Gustavsen,* "Wide band modeling of power transformers," IEEE Trans. Power Del., vol. 19, no. 1, pp. 414–422, Jan. 2004.
3. *G. B. Gharehpetian, H. Mohseni, and K. Moller,* "Hybrid modeling of inhomogeneous transformer windings for very fast transient overvoltage studies," *IEEE Trans. Power Del.*, vol. 13, no. 1, pp. 157–163, Jan. 1998.
4. *P. G. Mclaren and M. H. Abdel-Rahman,* "Modeling of large AC motor disk for steep-fronted surge studies," *IEEE Trans. Ind. Appl.*, vol. 24, no. 3, pp. 422–426, May/Jun. 1988.
5. *J. L. Guardado and K. J. Cornick,* "A computer model for calculating steep-fronted surge distribution in machine windings," *IEEE Trans. Energy Convers.*, vol. 4, no. 1, pp. 95–101, Mar. 1989.

6. *Y. Shibuya, S. Fujita, and N. Hosokawa,* "Analysis of very fast transient over voltage in transformer winding," *Proc. Inst. Elect. Eng., Gen. Transm. Distrib.*, vol. 144, no. 5, pp. 461–468, 1997.
7. *M. Popov, L. V. Sluis, and G. C. Paap,* "Computation of very fast transient over voltages in transformer windings," *IEEE Trans. Power Del.*, vol. 18, no. 4, pp. 1268–1274, Oct.. 2003.
8. *M. Popov, L. van der Sluis, R. P. P. Smeets, and J. Lopez Roldan,* "Analysis of very fast transients in layer-type transformer windings," *IEEE Trans. Power Del.*, vol. 22, no. 1, pp. 238–247, Jan. 2007.
9. *P.Ying and R. Jiagjum,* "Investigation of very fast transient overvoltage distributed in taper winding of tesla transformer," *IEEE Trans. Magn.*, vol. 42, no. 3, pp. 434–441, Mar. 2006.
10. *Guishu Liang, Haifeng Sun, Xile Zang, and Xiang Cui,* Modeling of Transformer Windings Under Very Fast Transient Overvoltages, IEEE Transactions on Power Delivery, vol. 48, no. 4, November, pp. 733 – 741 2006.
11. *D. J. Wilcox, M. Conlon, and W. G. Hurley,* "Calculation of self and mutual impedances for coils on ferromagnetic cores," *Proc. Inst. Elect. Eng.*, vol. 135, no. 7, pp. 470–476, Sep. 1988, h A.
12. *Gabriel Bonțidean, Florin Rezmeriță, Mihai Iordache, Neculai Galan,* „Simulations and experimental tests on the distribution of over-voltage within transformer windings"; SME'13 ninth edition, Bucharest, 2013.
13. *S. Fujita, N. Hosokawa, and Y. Shibuya,* "Experimental investigation of high frequency voltage oscillation in transformer windings," *IEEE Trans. Power Del.*, vol. 13, no. 4, pp. 1201–1206, Oct. 1998.
14. *M. Iordache, Lucia Dumitriu, D. Delion,* "SYSEG – SYmbolic State Equation Generation", User Guide, Electrical Department Library, Politehnica University of Bucharest, 2007.
15. Moraru A., Anghel Felicia, *Calculation of the voltage transient process in interleaved transformer coils*, Rev.Roum.Sci.Tech. Electrotechn. et Energ., 25, 3, 389-401, 1980
16. Heller B., Veverka A., *Die Modeltheorie der Stosserscheinungen in Transformatoren*, EuM, 11, 249, 1957
17. *M. Iordache, Lucia Dumitriu, I. Matei,* "ENCAP – Electrical Nonlinear Circuit Analysis Program", User Guide, Electrical Department Library, Politehnica University of Bucharest, 2000.
18. *M. Iordache, Lucia Dumitriu, I. Matei,* "SYMNAP – SYmbolic Modified Nodal Analysis Program", User Guide, Electrical Department Library, Politehnica University of Bucharest, 2002.
19. *N. Galan,* „Electrical machines", Romanian Academy Publishing House, Bucharest, 2011.
20. *Cezar Parteni Antoni P., Antoniu I.S.*, Comportarea maSinilor electrice la unda de Soc, Editura Academiei Române, 1957;